International Journal of Thin Films Science and Technology

http://dx.doi.org/10.12785/ijtfst/040311

Influence of Substrate Temperature on Physical Properties of Nanostructured Ti Doped In_2O_3 Thin Films by a Simplified Perfume Atomizer Technique

V. Sivaranjani and P. Philominathan[*]

PG and Research Department of Physics, AVVM Sri Pushpam College (an autonomous institution affiliated to Bharathidasan University, Trichy), Poondi, Thanjavur 613 503, India.

Received: 21 Mar. 2015, Revised: 22 May 2015, Accepted: 24 May 2015.
Published online: 1 Sep. 2015.

Abstract: Ti doped indium oxide thin films (I n2 O3 :Ti) were prepared at different temperatures by a simplified spray pyrolysis technique using perfume atomizer technique. The effect of substrate temperature on structural, electrical, photoluminesence and optical properties of these films have been analyzed and reported here. The XRD analysis revealed that the films possess polycrystalline with cubic bixbyite structure and the preferred orientation being in (2 2 2) direction. The grain size of the films varied from 31 nm to 55 nm with the increase of substrate temperature from 300o C to 400o C, thereafter it decreased with further increase of substrate temperature to 450° C. Optical parameters such as transmittance, absorption coefficient, refractive index and band gap have been studied and analyzed as a function of substrate temperature. Compared to other deposition temperatures (300o C, 400o C and 450o C) a film prepared at 350o C has exhibited a low electrical resistivity of 1.26 ×10−4 Ω cm, high mobility 66 cm2 /V s and carrier concentration 3.46 ×1020 cm−3 with 75 % of transmittance in the wavelength ranging between 400 nm - 1100 nm. An efficient photoluminescence emission was recorded for all the samples in the wavelength region of 300 nm - 600 nm which confirmed that these films are suitable for potential applicability in nanoscale optoelectronic devices.

Keywords: Thin film, Semiconductor, Electrical properties, X-ray diffraction.

1 Introduction

Significant interest has been generated during the past decades in preparing nanostructured oxides for various applications. Especially, the transparent conducting oxide (TCO) thin films have attracted much attention due to their wide range of applications in electro optical devices. However, a common problem in various TCO films like indium tin oxide (ITO), fluorine doped tin oxide and aluminum doped zinc oxide has been its high free carrier absorption in near infrared (NIR) region [1]. In the pursuit of improving the TCO films with good electrical conductivity and optical properties, many researchers [2-4] have succeeded in enhancing the carrier mobility rather than increasing the carrier concentration and the effort has been continuing to a larger extent, in recent times. Such improvised TCO films with high carrier mobility and low free absorption in the NIR with appropriate surface morphology, termed as transparent conducting light trapping oxides (TCLOs)[1,4-6]. Recently, the TCO thin films such as ITO, SnO_2 , CdO, ZnO etc., have taken the central stage and in particular the studies on I n2 O3 thin films find potential application in modern and opto electronics. Moreover, one-dimensional I n_2 O_3 nanostructures have been demonstrated to be sensitive to N O_2 and N H_3 gases [7-8] as well as to biomolecules [9]. I n_2 O_3 thin film has been used as active layers in ozone (O_3) gas sensors [10-12] and also used in solar cells, transparent electrodes for hetero-junction solar cells, liquid crystal display [13-14] and antireflection coatings for silicon solar cells [15-16]. Among the high mobility TCO films, Mo, W and Ti doped indium oxide thin films show excellent performance [17-19]. Their electron mobility changes from tens to hundreds (in units of cm^2 V^{-1} s^{-1}) depending on the deposition technique and processing parameters. Laboratory samples show higher mobility than those obtained from other deposition techniques, including magnetron sputtering, direct current sputtering, evaporation, channel spark ablation and hollow cathode sputtering [20-22]. In most deposition process, obtaining perfect crystallization and enhancing electron

[*]Corresponding author E-mail: philominathan@gmail.com

mobility involve maintaining the temperature of substrates at values higher than 300ºC.

Motivated by the above considerations, in this investigation, we wish to present the results of I n_2 O_3 :Ti thin films deposited by a simplified spray pyrolysis technique employing a perfume atomizer (which has not been reported yet). Here, we are investigating the effects of substrate temperature on the structural, electrical, photoluminescence and optical properties of I n_2 O_3: Ti thin films.

2 ExperimentalDetails

InCl3 (10 at. %), is the source of In and it was dissolved in 2ml of HCl with 30 ml of deionized water and appropriate quantity of TiCl4 (3 at. %) was dissolved in 15 ml of ethanol for titanium doping. The mixture of two solutions was stirred for an hour at atmospheric conditions and then sprayed manually on preheated glass substrates, using perfume atomizer method with various substrate temperatures (300o C , 350o C , 400o C and 450o C) and the concentration of starting material was kept constant. The perfume atomizer technique, introduced by Sawada et al., has been considered in the present study to deposit Ti doped indium oxide thin films, due to its manifold advantages [23-24].

All films were characterized by X-ray diffraction, UV-Visible spectroscopy, electrical measurement and photoluminescence spectroscopy. The X-ray diffraction (XRD) patterns were obtained using the computer controlled phillipsX'pertPRO XRD system (Cu Kα radiation; λ = 1.5405A) in Bragg - Brentano geometry. The electrical parameters were measured using a Hall measurement setup (Bio - Rad HL5500 Hall system) in Vander Pauw configuration with a permanent magnet of 5 kg. The optical transmittance (T) was measured using a UV-Visible-NIR spectrometer (Perkin elmerLamda 35). The photoluminescence spectra were carried out by spectroflurometer (JobinYvon- FLUROLOG FL3- 11) with Xenon lamp (450 w).

3 Results and Discussions

3.1 XRD analysis

Fig.1 shows the XRD patterns of Ti doped indium oxide thin films of different substrate temperatures and reveals that all the films were polycrysatlline with a cubic bixbyite indium oxide structure. Also, the patterns showed five well-defined peaks corresponding to (2 1 1), (2 2 2), (4 0 0), (4 4 0) and (1 0 3) diffraction planes of I n2 O3 . No peaks corresponding to titanium which was observed in the XRD patterns which is confirmed that there is no additional phase present in Ti doped indium oxide thin films. The intensities of all diffraction peaks were found to be high for a film deposited at350º C indicating a better cystallinity. Hence it may be considered as an optimum temperature to obtain uniform, well adherent Ti doped indium oxide thin films. The film deposited at 300o C, the intensity of diffraction peak is found to be low which confirmed the poor crystalline growth of the films on substrate surface due to insufficient thermal energy. The intensity of the peak shows a significant decrease as the substrate temperature increases from 400º C to 450º C. This indicates the deterioration of crystallinity and strain caused at high temperatures. As seen in Table.1, the thickness of the prepared films decrease with the increase in substrate temperature. The decrease in film thickness with substrate temperature may be attributed to the increase in evaporation rate of the initial product with increase indeposition temperature [25]. The size of crystallites oriented along (2 2 2) peak was calculated with the help of Scherrer's formula [26]. The microstrain, texture coefficient and crystalline size of the Ti doped indium oxide thin films were calculated from the following relations. The cyrstalline size, microstrain, texture coefficient and FWHM of the Ti doped indium oxide thin films are listed in Table.1

$$D = K\lambda/\beta\cos\theta \quad (1)$$

$$\varepsilon = \beta\cos\theta/4 \quad (2)$$

$$TC(hkl) = I_o(hkl)/I_s(hkl)\ \{1/N \sum[I_o(hkl)/I_s(hkl)]\}^{-1} \quad (3)$$

where k is the shape factor (0.9), λ is the wavelength of X-ray (1.5406 A), β is the FWHM of the high intensity peak [(2 2 2)], θ is the Bragg angle of XRD peak, ε is the microstrain, TC is the texture coefficient, I_O is the observed intensity, I_S is the standard intensity (JCPDS card no: 00-006-0416) and N is reflection number. The crysatllite size of the films increases from 31 nm to 55 nm with increase in substrate temperature from 300°C to 400°C, thereafter it slightly decreases with further increase of substrate temperature to 450° Cas seen Table.1. The crystallinity of these films with dependence of substrate temperature may be rendered as follows. When substrate temperature increases, the oxygen deficiency leads to the growth of less homogeneous films with more cyrstallographic faults. It suggests that the non-stoichiometric films show poor crystallinity [27]. The preferential or random growth of polycrystalline thin films can be understood by evaluating the texture coefficient TC (h k l) for all planes. It is clear from the definition that the deviation of texture coefficient from unity implies the film growth occurs in certain preferred orientation. The variation of the texture coefficients is given in Table.1, the higher value of texture coefficient at 350°c

Table 1: Various parameters of Ti doped indium oxide thin films, t-thickness, TC-Texture coefficient, and FWHM- Full width half maximum.

Substrate temp. (^{o}c)	t (nm)	TC (2 2 2)	FWHM (rad)	Grain size (nm)	Strain
300	260	1.30	0.26	31	1.09
350	146	1.35	0.21	39	0.88
400	97	1.27	0.15	55	0.63
450	68	1.25	0.36	22	1.15

However, the intensity of (2 2 2) peak has tendency to decrease with an increase in substrate temperature. This presumably is due to the strain occurring in the Ti doped indium oxide thin films. Therefore, the XRD analysis concluded that the film deposited at 350ºc has better crystallinity compared with other prepared films.

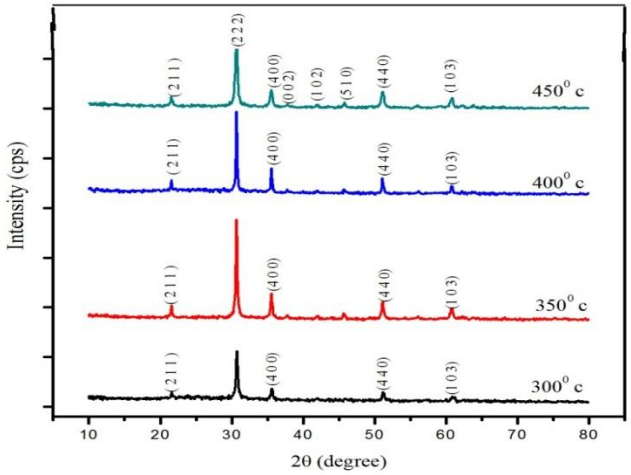

Figure 1: XRD patterns of Ti doped indium oxide thin films as a function of substrate temperatures.

3.2 Photoluminescence analysis

Fig. 2(a-d) shows the Photoluminescence (PL) spectra of Ti doped indium oxide thin films grown in the deposition temperatures in the range of 300º C to 450º C. The Photoluminescence spectra have been obtained at room temperature with excitation wavelength 350 nm for all deposited films. The well-defined peaks were observed in 412 nm, 468 nm and 550 nm (blue, violet and green band emission) when the samples excited with 350 nm. It is due to donor acceptor pair (DAP) transition between Ti vacancy and oxygen vacancy on an indium site [28-31]. Generally, in semiconductor materials the luminescence can be observed due to excitonic and trapped emissions. An excitonic emission is sharp and located near the absorption edge and trap state emission is broad and located at longer wavelength regions [32-33]. The low intensity peaks also observed in the PL spectra can be attributed to the inter impurity transitions and larger stoichiometric deviation in the films. All the films show a broad green emission in the visible region (550 nm), this emission peak was commonly referred to the deep level or trap state emissions due to the oxygen vacancies, similar results were found from the earlier report for I n2 O3 nanoparticles [34]. From the PL spectra the peaks were found to broaden with increase in substrate temperature and the inhomogeneous broadening of peaks can be attributed to high concentration of defects occur at high substrate temperature. The broad emissions are typical for the non-equilibrium process of film growth and caused by non-stoichiometry and metastable order and disorder on cation sublattice [35]. Further, the broadening of PL emission peaks obtained from the film deposited at 450º C was due to the fact that more defects present in that samples. These defects lead to non-radiative recombination [36]. These photoluminescence emission in the UV region at room temperature may found to be suited for optoelectronic devices.

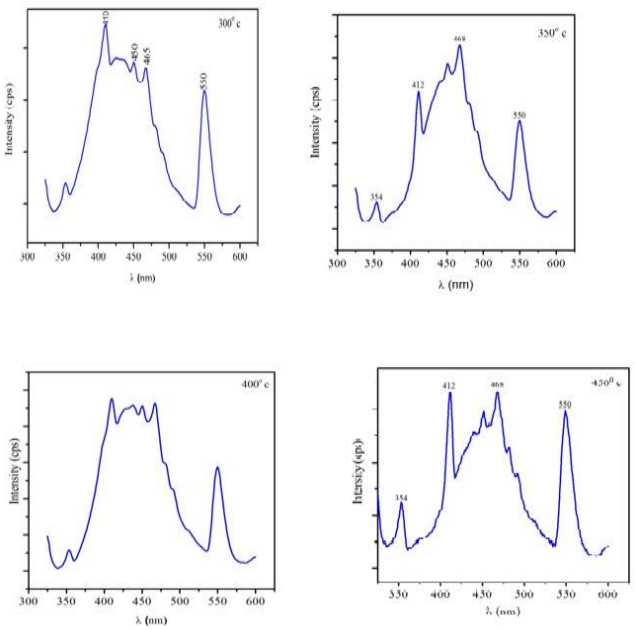

Figure 2: PL spectra of Ti doped indium oxide thin films for different substrate temperatures(a) 300ºC (b) 350ºC (c) 400ºC (b) 450ºC

3.3Electrical analysis

The resistivity, carrier concentration and mobility as a function of substrate temperature (300o C to 450o C) is shown in Fig. 3 and Fig. 4. The Hall measurements confirmed that all the prepared samples have n-type conductivity. The film deposited at 300o C exhibits a resistivity of 1.33 $\times 10^{-4}$ Ω cm, as the substrate temperature increases to 350o C, the resistivity decreases to a minimum value of 1.26 $\times 10^{-4}$ Ω cm, due to the improved Ti substitution in I n2O3 film crystallinity. Similar results were also obtained in Zr-doped I n2 O3 thin films [37]. At this temperature the mobility of the prepared film undergoes maximum which results in the greatly weakened carrier scattering process due to the improvement of crystallinity. The increase in both carrier concentration and mobility of these films due to the reduction of resistivity. The maximum value of carrier concentration and mobility (3.46 ×1020 cm^{-3} and 66 cm^2 /V s) obtained for a film prepared at 350o C. A further increase in substrate temperature causes degradation of the electrical properties. The increase of the film resistivity may be ascribed to both the reduction in the carrier concentration and carrier mobility. Hence, an increase of electrical resistivity should be attributed to the increase of the grain boundary scattering. As seen in Table.1, the crystalline size decreases with increase in substrate temperature (450ºC). Smaller crystalline size results in a higher density of grain boundaries, which acts as barriers for carrier transport and traps for free carriers. Hence, a decrease of crystalline size causes an increase of grain boundary scattering [38]. The decrease of carrier concentration may be due to the decrease of native donors resulted from the enhancement of oxidation on the substrate surface [39]. Moreover, an increase in chemisorped oxygen which act as an electron traps decrease of carrier concentration [40]

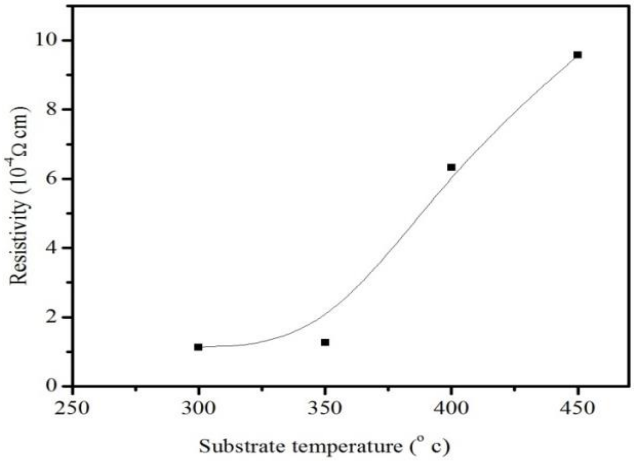

Figure 3: Variation of resistivity as a function of substrate temperatures for Ti doped indium oxide thin films

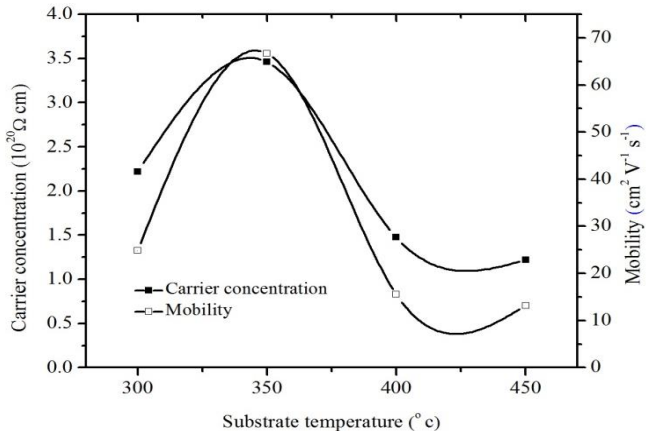

Figure 4: Variation of carrier concentration and mobility as a function of substrate temperatures

3.4 Optical analysis

Fig. 5 shows the transmittance spectra of the Ti doped indium oxide thin films measured in the range of 300-1100 nm. The film deposited at 350º C showed high transmittance of 75 % , while the film prepared at higher substrate temperature (450º C) exhibited the lowest transmittance of 59 % in the visible to NIR region compared to the other films. The decrease in transmittance at higher substrate temperature may be attributed to the scattering of photons with surface of film and also due to the conversion of crystalline to non-crystalline with the increase of substrate temperature.

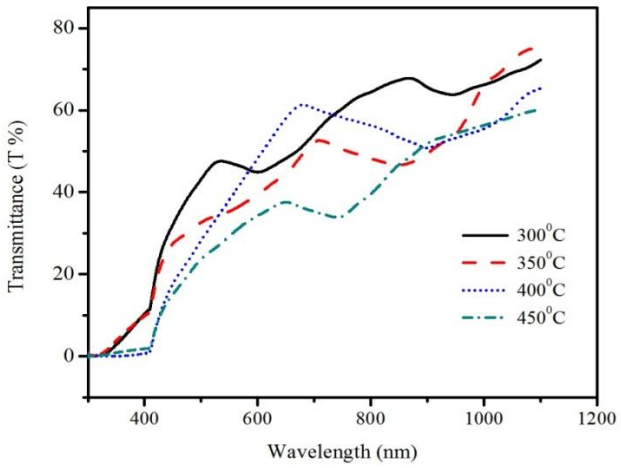

Figure 5: Transmission spectra of Ti doped indium oxide thin films for various substrate temperatures.

The absorption coefficient is an important parameter for characterizing the penetration depth of the light wave into the thin film layer. The absorption coefficient and refractive index of Ti doped indium oxide thin films were obtained employing the algorithm by E.G. Birgin et al., [41]

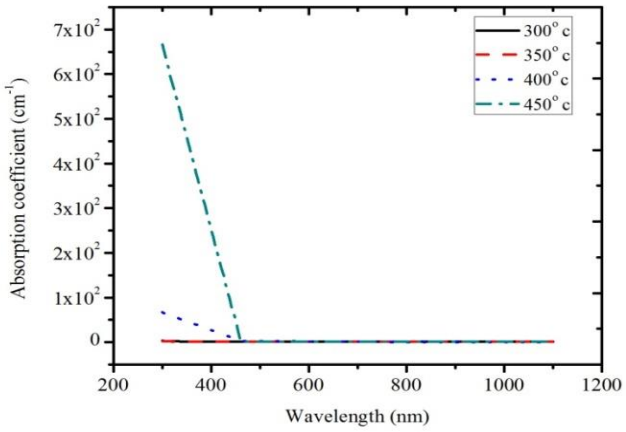

Figure 6: Response of Absorption spectra of Ti doped Indium Oxide thin films for various substrate temperatures

The absorption coefficient spectra for different substrate temperatures was depicted in Fig. 6. The absorption coefficient of the films deposited at 300ºC and 350ºC is almost zero which may be due to the maximum transmission in the region of 340 nm to 1100 nm. Compared to other substrate temperatures, the films deposited at 400oC and 450oC show higher absorption coefficient values of 1 ×102 cm−1 and 7 ×102 cm^{-1}respectively in the wavelength range of 300-460 nm, then they fall down sharply towards higher wavelengths. From these results we concluded that in this region (Visible-NIR region), the prepared samples have maximum transmittance as shown in transmission spectra. The optical band gap of the films calculated from the transmittance spectra by applying Tauc's model [42]:

$$\alpha h\upsilon = A(E_g - h\upsilon)^n \quad (4)$$

where Eg is the optical band gap, hν is the incident photon energy and B is the constant and n can have values 1/2, 3/2, 2 and 3 depending upon the mode of inter band transition, i.e. direct allowed, direct forbidden, indirect allowed and indirect forbidden transition respectively. For n=1/2 the transition data provide the best linear curve in the band edge region, which shows that the transition is direct in nature. The band gap of the prepared films were calculated using Tauc's plot by plotting $(\alpha h\nu)^2$versus hν , and the variation of band gap as a function of substrate temperature is shown in Fig. 7. In this investigation, when substrate temperature increases from 300º C to 450º C, the value of the optical band gap gradually decreases from 3.75 eV to 3.25 eV. Therefore the optical band gap decreases with increase in carrier concentration for substrate temperature kept at 300o C and 350o C, thereafter carrier concentration slightly decrease with further increase of substrate temperatures from 400ºC to 450oC. Generally, defects are aggregated at the grain boundaries. Smaller grain size results in a tensile strain arising from thermal mismatch between the deposited films and the substrate, which indicates that the presence of large number of grain boundaries increases the defects in the film. The defects could act as the radiative recombination centers that emit visible light and cause transition to lower band and results in the reduction of band gap [43]. According to Burstein-Moss effect, raising the Fermi level into the conduction band of degenerate semiconductor leads to energy band broadening [44]. In this study the results of optical band decreases with increase in substrate temperature from which we can conclude that the Burstien -Moss effect is weak. Therefore, shrinkage effect is dominant over the Burstein-Moss effect, since the Eg values decreases with the increase of deposition temperature.

The refractive index of the films deposited on glass substrate with various deposition temperatures as shown in Fig. 8 and higher value of refractive index was obtained for films deposited at 300o C and 450o C respectively. The variation of the refractive index with substrate temperature may be correlated with the density of the films. At 450º C, the refractive index has maximum value and then it gradually decreases for the films deposited at 300º C, 350º c and 400º C. The reason for the lowering refractive index of these films is that it has relatively low packing density. Lowering of the packing density is caused by the incorporation of oxygen during the film growth [45], which may create voids that absorb moisture [46]. Moreover, collisions of the evaporated species with O2 molecules reduce their kinetic energy before reaching substrate and this will result in lower packing density [46]. The increase of refractive index with substrate temperature may be attributed to an increase in the density of films deposited on heated substrates. Further the refractive index of the films vary inversely with transmission. The high (low) transmittance spectra has low (high) optical constants [47].

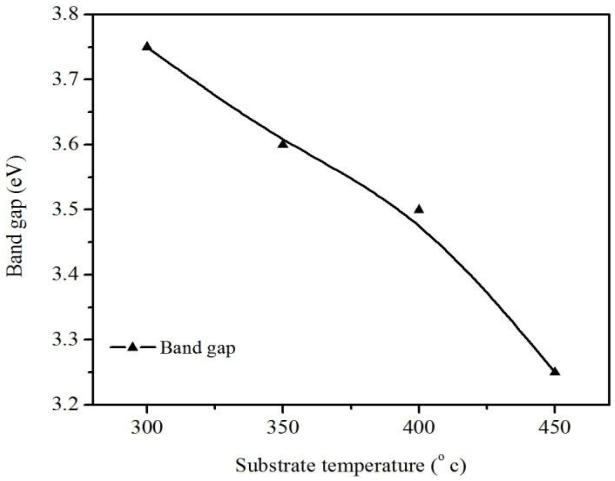

Figure 7: Optical band gap of Ti doped indium oxide thin films as a function of substrate temperatures.

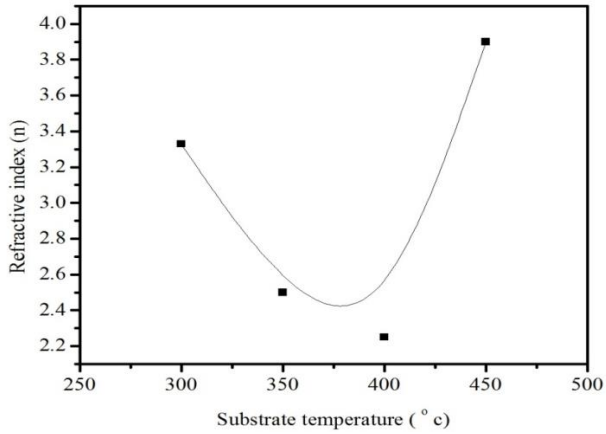

Figure 8: Refractive index of Ti doped indium oxide thin films for different substrate temperatures

4. Conclusion

In this present investigation the effect of substrate temperature on structural, photoluminescence, optical and electrical properties of the deposited Ti doped indium oxide thin films prepared by a perfume atomizer method has been studied. The X-ray diffraction analysis of these films revealed that the deposited samples have polycrystalline structure for the temperature range (300° C - 450° C) with a preferred orientation along (2 2 2) lattice plane instead of (4 0 0) reflection plane. The lowest resistivity achieved is 1.26×10^{-4} Ω cm with a high mobility of 66 cm2 /V s for the film deposited at 350o C. The optical constants such as refractive index, absorption coefficient and band gap were obtained from the transmission data. The photoluminescence spectra of Ti doped indium oxide thin films exhibit well defined broad emission peaks corresponding to defect related luminescence emissions.

Acknowledgment

One of the authors V. Sivaranjani acknowledges the financial support pro- vided by UGC New Delhi in the form of Rajiv Gandhi National Fellowship (F1-17.1/20112012/RGNFSCTAM438/(SAIII/Website)dt.06.06 .2012.The corresponding author acknowledges UGC New Delhi for the assistance through MRP (F.No.41-961/2012 (SR) dt.26.07.2012).

References

[1] J.A. Anna Selvan, A.E. Delahoy, S. Guo& Y. Li, Sol. Energy Mater. Sol. C, 90 (2006) 3371.

[2] E. Elangoven, G. Goncalves, R. Martins & E. Fortunato, Sol. Energy Mater. Sol. Cells, 83 (2009) 726.

[3] Y. Meng, X.L. Yang, H.X. Chen, J. Shen, Y.M. Jiang, Z.J. Zhang, Z.Y. Hua, Thin Solid Films 394 (2001) 218.

[4] Y. Yoshidaa, T.A. Gessert, C.L. Perkins, T.J. Coutts, J. Vac. Sci. Technol. A 21 (2003) 1092

[5] D. Cahen, A. Kahn & E. Umbach, Mater. Today, 8 (2005) 32.

[6] E. Fortunato, D. Ginley& H. Umbach, Mater. Res. Bull., 32 (2007) 1.[7] Zh. Pan, Z. Dai, Z.L. Wang, Science 291 (2001) 1947.

[8] W.S. Seo, H.H. Jo, K. Lee, J.T. Park, Adv. Mater. 15 (2003) 795.

[9] C. Li, D. Zhang, X. Liu, S. Han, T. Tang, J. Han, C. Zhou, Appl. Phys. Lett. 82 (2003) 1613.

[10] K. Soulantica, L. Erades, M. Sauvan, F. Senocq, A. Maisonnat, B. Chau- dret, Adv. Funct.Mater.13 (2003) 553.

[11] C. Li, B. Lei, D. Zhang, X. Liu, S. Han, T. Tang, M. Rouhanizadeh, T.Hsiai, C. Zhou, Appl. Phys. Lett.83 (2003) 4014.

[12] X. Li, M.W. Wanlass, T.A. Gessert, K.A. Emery, T.J. Coutts, Appl. Phys. Lett. 54 (1989) 2674.

[13] K. Srinivas, T. Sudersena Rao, A. Mansingh, J. Appl.Phys.57 (1985) 384.

[14] Y. Shigesato, S. Thalaki, T. Haranob, J. Appl. Phys. 71 (1992) 3356.

[15] D. Beena, K.J. Lethy, R. Vinodkumar, V.P. Mahadevan Pillai, Solar Energy Mater. Solar Cells 91 (2007) 1438.

[16] A. Salehi, Thin Solid Films 324 (1998) 214.

[17] M. Anwar, I.M. Ghauri, S.A. Siddiqi, J. Mater. Sci. 41 (2006) 2859. [18] Y. Abe, N. Ishiyama, Mater. Lett.61 (2007) 566.

[19] M.F.A.M. Van Hest, M.S. Dabney, J.D. Perkins, D.S. Ginley, M.P. Taylor, Appl. Phys. Lett.87 (2005) 032111.

[20] P.F. Newhouse, C.H. Park, D.A. Keszler, J. Tate, P.S. Nyholm, Appl. Phys. Lett. 87 (2005) 112108.

[21] R.K. Gupta, K. Ghosh, R. Patel, P.K. Kahol, Appl. Surf.Sci. 255 (2008) 3046.

[22] R.K. Gupta, K. Ghosh, S.R. Mishra, P.K. Kahol, Mater. Lett.62 (2008) 1033.

[23] Y. Sawada, C. Kobayashi, S. Seki & H. Funakibo, Thin Solid Films, 409 (2002) 46-50.

[24] K. Ravichandran. And P. Philominathan: Sol.Energy, 82 (2008) 1062-1066 [25] B.J. Lokhande, M.D. Uplane, Mater. Res. Bull. 36 (2001) 439-447.

[26] K. Venkateswarlu, A. Chandra Bose, N. Rameshbabu, Physica B 405 (2010) 4256-4261.

[27] R. Romero, D. Leinen, E.A. Dalchiele, J.R. Ramos Barrado, F. Martin, Thin Solid Films 515 (2006) 1942-1949.

[28] J.J.M. Binsma, L.J. Giling, J. Bloem, J. Lumin. 27 (1982) 35.

[29] J. Van Gheluwe, J. Versluys, D. Poelman, J. Verschraegen, M. Burgelman, P. Clauws, Thin Solid Films 511512 (2006) 304308.

[30] J. Eberhardt, H.Metzner, R. Goldhahn, F. Hudert, U.Reislohner, C. Hulsen, J. Cieslak, T.H. Hahn, M. Gossla, A. Dietz, G. Gobsch, W. Wit- thuhn, Thin Solid Films 480481 (2005) 415.

[31] M. Nanu, J. Schoonman, A. Goossens, Thin Solid Films 451452 (2004) 19. [32] Y.J. Hsu, S.Y. Lu, Y.F. Lin, Adv. Funct. Mater.15 (2005) 1350.

[33] M. O Neil, J. Marohn, G. Melendon, J. Phys. Chem. 94 (1990) 4356. [34] H.J. Zhou, W.P. Cai, L.D. Zhang, Appl. Phys. Lett.75 (1999) 495.

[35] H. Metzner, Th. Hahn, J.-H.Bremer, M. Seibt, B. Plikat, I. Dirnstorfer, B.K. Meyer, Thin Solid Films 361362 (2000) 504508.

[36] B.A. Kulp, H. Kelley, J. Appl. Phys. 31 (1960) 1057.

[37] H. Kim, J.S. Horwitz, G.P. Kushto, S.B. Qadri, Z.H. Kafafi, D.B. Chrisey, Appl. Phys. Lett.78 (2001) 10501052.

[38] H. Kim, J.S. Horwitz, G. Kushto, A. Pique, Z.H. Kafafi, C.M. Gilmore, D.B. Chrisey, J. Appl. Phys. 88 (2000) 60216025.

[39] X.Q. Gu, L.P. Zhu, Z.Z. Ye, Q.B.Ma, H.P.He, Y.Z. Zhang, B.H. Zhao, Sol. Energy Mater. Sol. Cells 92 (2008) 343347.

[40] Q.B. Ma, Z.Z.Ye, H.P.He, L.P. Zhu, W.C. Liu, Y.F. Yang, L.Gong, J.Y. Huang, Y.Z. Zhang, B.H. Zhao, J. Phys. D: Appl. Phys.41 (2008) 055302055306.

[41] E. G. Birgin, I. Chambouleyron, and J. M. Martnez, Journal of Computa- tional Physics 151, 1999 862-880.

[42] D. Jiles, Introduction to the Electronic Properties of Materials, Chapman and Hall, New York, 1994, p. 180.

[43] K.P. Bhuvana, J. Elanchezhiyan, N. Gopalakrishnan, T. Balasubramanian, Mater, Sci. Semicond Process. 14 (2011) 8488.

[44] Q.B. Ma, Z.Z. Ye, H.P.He, L.P. Zhu, J.Y. Huang, Y.Z. Zhang, B.H. Zhao, Scripta Mater. 58 (2008) 2124.

[45] R. Thielsch, A. Gatto, J. Heber, N. Kaiser, Thin Solid Films 410 (2002) 86.

[46] H. Hu, C. Zhu, Y.F. Lu, Y.H. Wu, T. Liew, M.F. Li, B.J. Cho, W.K. Choi, J. Appl. Phys. 94 (2003) 551.

[47] A. AbdolahzadehZiabari, F.E. Ghodsi, J. Mater. Sci.: Mater. Electron.23 (2012) 1639.